

27 ratio. The results of the present-day calculations suggest a certain amount of parameter refinement
28 is still needed to reconcile the updated chemistry with field observations (particularly for
29 HO₂+RO₂). However, the updated chemistry could have far-reaching implications for: future-
30 climate predictions; projections of future oxidising capacity; and our understanding of past changes
31 in oxidising capacity.

32

33

34 **1.0: Introduction.**

35 Isoprene (2-methyl-1,3-butadiene) emissions comprise a major fraction of total biogenic volatile
36 organic compound (BVOC) emissions. Field and modelling studies estimate that the natural
37 emissions of isoprene have been fairly constant over the last decade or so, ~400-500 Tg C/yr
38 [Müller et al., 2008]. Owing to the high reactivity of isoprene towards the hydroxyl radical (OH),
39 model studies invariably implicate isoprene as a large sink of OH. However, the reactive products
40 formed from the oxidation of isoprene by OH, the isoprene hydroxy-peroxy radicals (ISOPHO₂),
41 can interact with oxides of nitrogen (NO_x = NO+NO₂) resulting in production of ozone in the
42 troposphere—the main OH precursor.

43 Recent field studies in major isoprene emitting regions such as Amazonia [Lelieveld et al., 2008]
44 and South East Asia [Hewitt et al., 2010] have found large discrepancies between modelled and
45 measured HO_x concentrations. These discrepancies are not confined to the tropics, but coincide with
46 regions impacted by isoprene emissions [Hofzumahaus et al., 2009; Tan et al., 2001]. The model-
47 measurement disagreement is most pronounced where high isoprene concentrations (> 1 ppbv)
48 coincide with low NO_x concentrations (< 1 ppbv). Several theoretical [Peeters et al., 2009; Peeters
49 and Müller 2010; da Silva et al., 2010] and experimental [Paulot et al., 2009] studies have recently
50 provided new insights into the oxidation mechanism of isoprene. No doubt, more studies will be
51 required to unravel its intricacies. However, the work of Peeters et al. [2009] concerning
52 unimolecular reactions of ISOPHO₂, has been shown in both box model [Archibald et al., 2010]

53 and global models [Archibald et al., 2010; Stavrakou et al., 2010] to improve the representation of
54 low-NO_x isoprene chemistry.

55

56 We use the UKCA global chemistry-climate model (<http://www.ukca.ac.uk>) to explore the impact of
57 including isomerisation reactions of ISOPOHO₂ on the composition of the atmosphere in the
58 present (2000), pre-industrial (*ca.* 1850) and future (2100). There exists a great deal of work in the
59 literature about the importance of isoprene oxidation in global chemistry [e.g. Wang and Shallcross,
60 2000], and more recently, a great deal of debate towards the issues of reconciling problems with
61 representing its chemistry in global models [Lelieveld et al., 2008; Archibald et al., 2010; Stavrakou
62 et al., 2010]. There are likely to be modifications to the mechanism of isoprene oxidation as time
63 progresses, but this work investigates the most important aspect that has been thus far poorly
64 represented – the regeneration of HO_x radicals through isomerisation reactions of ISOPOHO₂.

65

66

67 **2.0: Method.**

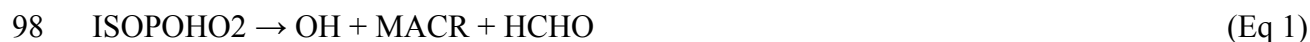
68 A number of experiments with the UKCA model, run at a horizontal resolution of 3.75° in longitude
69 × 2.5° in latitude on 60 hybrid height levels that stretch from the surface to ~84 km, were carried
70 out. The model set up is similar to that described in Telford et al. [2010], with a chemical
71 mechanism comprising 60 chemical tracers and 132 photochemical reactions, including the
72 oxidation of isoprene based on the Mainz Isoprene Mechanism [Pöschl et al., 2000]. The model's
73 dynamical core is based on the Met Office's Unified Model version 6.1. In each experiment, the
74 model is allowed to run freely with the climate forced by specified concentrations of long-lived
75 greenhouse gases and ozone-depleting substances, in addition to prescribed sea surface
76 temperatures and sea-ice coverage from the HadISST dataset [Rayner et al., 2003]. Stratospheric
77 chemistry is not calculated explicitly. Instead, the concentrations of ozone and NO_y above 30 hPa
78 are taken from the Cambridge 2D model [Law and Pyle, 1993] and are not changed between

79 experiments, so that the influence of the stratosphere on the troposphere remains constant. The
80 results are taken from three-year integrations following an 18 month ‘spin-up’ period.

81

82 Our modifications to the isoprene mechanism follows that applied in the global model STOCHEM,
83 in the study of Archibald et al. [2010] (their reactions R24-R26). However, the representation used
84 in this study differs somewhat from Archibald et al. [2010] as we omit the formation of the
85 (predicted) highly photolabile hydroperoxy-aldehyde (HPALD) and instead assume prompt
86 formation of OH from both isomerisations of the ISOPOHO2. The two reaction pathways are
87 represented by Eq. 1 and 2 ($k_1 = 4.0 \times 10^{-3} \text{ s}^{-1}$; $k_2 = 8.0 \times 10^{-2} \text{ s}^{-1}$; MACR=lumped C4 carbonyl;
88 MGLY=methyl glyoxal; HACET=hydroxyacetone). The product yields were determined by running
89 a series of box model experiments and optimising the product yields to give a reasonable match to
90 the results of Mechanism 4 of Archibald et al. [2010] for HO_x, ozone and CO. The values used for
91 k_1 and k_2 come from Archibald et al. [2010], derived for conditions appropriate for the tropics. Both
92 k_1 and k_2 are predicted to have significant temperature dependence (Peeters and Müller [2010]
93 predict variations of up to a factor of 3 for a 10 K change in temperature). However, owing to the
94 fact that most isoprene is oxidised in the tropics (near the surface) where there is small variation in
95 temperature, it is expected that this simplification should have only a relatively small impact on the
96 results.

97



100

101 Six experiments were carried out: a Base run (B) and a Modified run (M; including the
102 isomerisation reactions of ISOPOHO2) each subject to Present-Day (PD), Pre-Industrial (PI) and
103 Future (FC) climate/emissions scenarios (see Table 1 for a breakdown of the emissions), based on
104 the emissions of Stevenson et al. [2006], Lamarque et al. [2010] and Dentener et al. [2005]

105 respectively. The future emissions reflect the IPCC B2+CLE scenario. Note the relatively similar
106 total BVOC emissions, but much lower total NO_x emissions, in the pre-industrial, compared with
107 the present. In all cases the amount of CH₄ is prescribed (Table 1). In each period, we assessed the
108 impact of the updated isoprene scheme in terms of absolute differences (i.e. M-B) and percentage
109 differences (i.e. $100 \times ((M-B)/B)$). We assessed the changes in the troposphere only and define this
110 layer based on the lapse rate.

111

112 **3.0: Results.**

113

114 **3.1: Present day.**

115 In general our base present-day simulation (PD-B) generates results for ozone and CO that are
116 consistent with a wide range of observations and compare well with other global models (Fig 1)
117 [c.f. Stevenson et al., 2006; Shindell et al., 2006]. A comparison against ozone-sonde measurements
118 is shown in Fig 1a (PD-B indicated by red line and pink envelope). In general, and in line with the
119 majority of models [e.g. Shindell et al., 2006], the PD-B simulation tends to under-predict CO in the
120 Northern Hemisphere and slightly over predict CO in the Southern Hemisphere (red line in Fig 1b).
121 Including the ISOPHO2 isomerisation reactions (PD-M, indicated by blue line and purple
122 envelope in Fig 1a) leads to an improvement in the comparison with ozone for almost all latitude
123 and pressure bands (the exception being Equator-30°N, 750hPa). Likewise, there is improved
124 simulation of CO and the SH high bias is slightly reduced in the PD-M simulation (blue line in Fig
125 1b). The levels of OH and HO₂ are enhanced by as much as 410% and 225% respectively in certain
126 regions at the surface and up to 75% in the zonal mean (Fig 2). These enhancements are
127 approaching those needed to reproduce the high concentrations of OH and HO₂ measured in the
128 tropics [Lelieveld et al., 2008]. Note that the greatest increases in OH are mainly limited to surface
129 regions in the tropics, where there are high emissions of isoprene but low emissions of NO_x. Fig 2d
130 clearly shows that surface increases are propagated throughout the tropical free troposphere. These

131 increases in the free troposphere are driven by convection in the tropics lifting the products of
132 isoprene oxidation (such as MGLY in Eq 2) to higher altitudes where rapid photolysis allows
133 enhanced production of HO₂. In our parameterisation of the products of the ISOPHO2
134 isomerisation's MGLY is included as a major product. Our PD-M simulation tends to predict
135 concentrations of MGLY which are comparable but higher (around a factor of two) than those
136 reported by Fu et al. [2008]. The exact products following ISOPHO2 isomerisation's are in need
137 of experimental verification. However, our representation of them as small oxidised compounds
138 known to be associated with isoprene oxidation should, to first order, have only a small effect on the
139 results.

140

141 In Fig 1c we compare modelled and measured OH and HO₂+RO₂ made during the OP3 campaign in
142 Borneo [Hewitt et al., 2010]. The PD-M simulation (blue line) clearly improves the comparison
143 between modelled and measured OH. Reducing the rate of the ISOPHO2 isomerisation's by a
144 factor of two (green lines) leads to a very small decrease in the OH enhancement compared with the
145 PD-M run. However, it is apparent from analysis of the HO₂+RO₂ data that some form of parameter
146 refinement is needed as the PD-M mechanism over simulates the amount of HO₂+RO₂ by more than
147 a factor of two. We note that this is not unique to our implementation of the Peeters' mechanism;
148 both Stavrakou et al. [2010] and Whalley et al. [2011 in prep] also present results that show an over-
149 simulation of HO₂ relative to OH. Globally, the amount of OH in the troposphere increases
150 significantly (Table 2) leading to a decrease in the lifetime of methane, of around 14%. The amount
151 of ozone also increases by some 25 Tg (8%) globally. This is driven by a reduction in the flux of
152 ozonolysis and by an increase in the flux through the reaction between HO₂ and NO. The level of
153 enhancement in HO_x in the present study is much greater than that reported by Archibald et al.
154 [2010] where at most they calculated increases of ~50%. This can be attributed to an overestimation
155 in that study of NO_x in isoprene rich areas, with the present results being more in line with the work
156 of Peeters and Müller [2010] and Stavrakou et al. [2010].

157

158

159 **3.2: Pre-industrial.**

160 As in previous studies [Mickley et al., 2001; Lamarque et al., 2005], our base pre-industrial
161 calculations (PI-B) cannot reproduce the very low concentrations of surface ozone measured at the
162 turn of the 20th century using the Schonbein method [Pavelin et al., 1999]. Mickley et al. [2001]
163 suggested this could be the result of an overestimation of NO_x emissions at that time. They also
164 postulated that increased emissions of reactive BVOCs could contribute, although Lamarque et al.
165 [2005] have subsequently argued that this would be inconsistent with our best estimates of PI
166 emissions. More recently, Pavalla et al. [2010] have reported that the inclusion of tropospheric
167 halogen chemistry can help to resolve this.

168

169 Like Mickley et al. [2001], we find that the combination of low levels of NO_x and the propensity for
170 isoprene to react with OH leads to near titration of OH in much of the continental boundary layer in
171 the tropics and mid-latitudes in our PI-B experiment. When we include the updates to the chemistry
172 (PI-M), as with the present-day, we calculate significant enhancements in OH and HO₂, but in the
173 pre-industrial this is to a much greater extent owing to the lower levels of NO_x. We calculate
174 enhancements in OH approaching 1500% in some regions at the surface, and 170% in the zonal
175 mean (in the tropics near the surface, see Fig 2); HO₂ is enhanced by as much as 300% at the
176 surface and 75% in the zonal mean. Enhanced destruction of CO in the boundary layer leads to
177 lower levels of CO, and higher levels of OH, throughout much of the troposphere. Globally, the
178 increase in OH leads to a 35% reduction in the lifetime of methane—a very substantial
179 decrease—whilst we calculate an increase in global ozone burden of 36 Tg (18%).

180

181

182 **3.3: Future.**

183 We explored a reasonably optimistic future-emissions scenario (IPCC B2+CLE), in which NO_x
184 emissions decrease but VOC emissions increase. We note that the increased emissions of isoprene
185 do not reflect the important role that CO₂ inhibition may play in a CO₂-warmed future [Young et al.,
186 2009]. The results of the base simulation (FC-B) are generally similar to the PD-B simulation,
187 although we simulate an increase in ozone of ~32 Tg. Similarly, on updating the chemistry (FC-M)
188 we calculate enhancements in OH and HO₂ of as much as 550% and 200% respectively at the
189 surface and greater than 75% for OH in the tropics near the surface as a zonal mean (see Fig 2). The
190 increased HO_x then leads to further increases in ozone burden (32 Tg or ~9%) and a significant
191 reduction in the lifetime of methane of ~11%.

192

193 **4.0: Discussion and conclusions.**

194 Implementing updated (low NO_x) chemistry for isoprene has led to large increases in modelled HO_x
195 concentrations. These increases are largest within the boundary layer in regions where NO_x
196 concentrations are low and isoprene concentrations are high. These areas are predominantly found
197 in the tropics. Deep convection in these areas lifts the products of isoprene oxidation into the free
198 troposphere and promotes ozone production (mainly through an increase in the reaction between
199 HO₂ and NO). Ultimately, the modified isoprene chemistry is sensitive to the chemical environment
200 which can be characterised on a global scale by the ratio of VOC/NO_x emissions. Characterising the
201 global effects of this modified chemistry by comparing relative changes in the methane lifetime
202 shows that there is a tailing off in the importance of the effect, from the pre-industrial to a warmer,
203 “cleaner” future. However, the importance of understanding the evolution in atmospheric
204 composition should not be underestimated. The changes in ozone burden (Table 2) (and to a lesser
205 extent methane lifetime) have bearings on future-climate predictions, owing to the radiative-forcing
206 properties of these greenhouse gases, whilst the changes in methane lifetime have consequences for
207 projections of future oxidising capacity, and our understanding of past changes in oxidising
208 capacity—an area we intend to explore further. The Peeters mechanism [Peeters et al., 2009] is

209 unlikely to be the last word on the subject but its contribution to our understanding of the chemistry
210 surrounding isoprene oxidation at low-NO_x concentrations has potentially far-reaching implications.
211 These warrant further study and validation via model-measurement comparison and crucially
212 targeted laboratory experiments aimed at simulating the conditions encountered in the tropical
213 boundary layer.

214

215

216 **Acknowledgments.**

217 We thank two anonymous referees for their comments of the original manuscript. ATA, NLA, PJT
218 and JAP thank NCAS climate for funding. JGL's contribution comprises part of the British
219 Antarctic Survey Polar Science for Planet Earth Programme, he gratefully acknowledges the NERC
220 for its support. PSM, AK, LKW, PME and DEH thank the NERC OP3 project (NE/D002192/1) and
221 NCAS FGAM for funding. DES and MEJ also acknowledge funding from NERC QUEST
222 (QUAAC and Deglaciation). We also thank Dr Paul Young for help in preparing the ozone
223 comparison figure.

224

225 **References.**

226 Archibald, A.T., et al., (2010), Impacts of mechanistic changes on HO_x formation and recycling in
227 the oxidation of isoprene, *Atmos. Chem. Phys.*, 10, 8097-8118, doi:10.5194/acp-10-8097-2010.

228 Dentener, F., et al., (2005), The impact of air pollutant and methane emission controls on
229 tropospheric ozone and radiative forcing: CTM calculations for the period 1990-2030, *Atmos.*
230 *Chem. Phys.*, 5, 1731-1755, doi:10.5194/acp-5-1731-2005.

231 Fleming, Z. L., et al., (2006), Peroxy radical chemistry and the control of ozone photochemistry at
232 Mace Head, Ireland during the summer of 2002, *Atmos. Chem. Phys.*, 6, 2193–2214,
233 doi:10.5194/acp-6-2193-2006. Fu, T.-M et al., (2008) Global budgets of atmospheric glyoxal and
234 methylglyoxal, and implications for formation of secondary organic aerosols, *J. Geophys. Res.*, 113,

235 D15303, doi:10.1029/2007JD009505.

236

237 Hewitt, C.N., et al., (2010), Overview: oxidant and particle photochemical processes above a south-
238 east Asian tropical rainforest (the OP3 project): introduction, rationale, location characteristics and
239 tools, *Atmos. Chem. Phys.*, 10, 169-199, doi:10.5194/acp-10-169-2010

240 Hofzumahaus, A., et al., (2009), Amplified trace gas removal in the troposphere, *Science*, 324,
241 1702-1704, doi:10.1126/science.1164566.

242 Horowitz, L. W. (2006), Past, present, and future concentrations of tropospheric ozone and aerosols:
243 Methodology, ozone evaluation, and sensitivity to aerosol wet removal, *J. Geophys. Res.*, 111,
244 D22211, doi:10.1029/2005JD006937.

245 Law, K., and J. Pyle (1993), Modeling Trace Gas Budgets in the Troposphere 1. Ozone and Odd
246 Nitrogen, *J. Geophys. Res.*, 98(D10), 18377-18400.

247 Lamarque, J.-F., et al., (2010), Historical (1850–2000) gridded anthropogenic and biomass burning
248 emissions of reactive gases and aerosols: methodology and application, *Atmos. Chem. Phys.*, 10,
249 7017-7039, doi:10.5194/acp-10-7017-2010.

250 Lamarque, J.-F., et al., (2005), Tropospheric ozone evolution between 1890 and 1990, *J. Geophys.*
251 *Res.*, 110, D08304, doi:10.1029/2004JD005537.

252 Lelieveld, J., et al., (2008), Atmospheric oxidation capacity sustained by a tropical forest, *Nature*,
253 452, 737–740, doi:10.1038/nature06870.

254 Logan, J.A., (1999), An analysis of ozonesonde data for the troposphere: Recommendations for
255 testing 3-D models, and development of a gridded climatology for tropospheric ozone, *J. Geophys.*
256 *Res.*, 104, 16,115–16,149.

257 Mickley, L., D. Jacob, and D. Rind (2001), Uncertainty in preindustrial abundance of tropospheric
258 ozone: Implications for radiative forcing calculations, *J. Geophys. Res.*, 106(D4), 3389-3399.

259 Müller, J.-F., et al., (2008), Global isoprene emissions estimated using MEGAN, ECMWF analyses
260 and a detailed canopy environment model, *Atmos. Chem. Phys.*, 8, 1329-1341, doi:10.5194/acp-8-

261 1329-2008.

262 Novelli, P.C., et al., (1998), Distributions and recent changes of carbon monoxide in the lower
263 troposphere, *J. Geophys. Res.*, 103(D15), 19,015–19,034.

264

265 Parella J.P., et al., (2010), Improved simulation of preindustrial surface ozone in a model with
266 bromine chemistry. AGU Fall Meeting, abstract #A31F-04.

267 Paulot, F., et al., (2009), Unexpected epoxide formation in the gas-phase photooxidation of
268 isoprene, *Science*, 325, 730–733, doi:10.1126/science.1172910.

269 Pavelin, E.G., et al., (1999), Evaluation of pre-industrial surface ozone measurements made using
270 Schonbein's method, *Atmos. Environ.*, 33, 919-929.

271 Peeters, J., T.L. Nguyen, and L. Vereecken, (2009) HO_x radical regeneration in the oxidation of
272 isoprene, *Phys. Chem. Chem. Phys.*, 11, 5935–5939, doi:10.1039/b908511d.

273 Peeters J. and J.-F., Müller (2010), HO_x radical regeneration in isoprene oxidation via peroxy
274 radical isomerisations. II: experimental evidence and global impact, *Phys. Chem. Chem. Phys.*, 12,
275 14227-14235, doi:10.1039/c0cp00811g

276 Pöschl, U., et al., (2000), Development and intercomparison of condensed isoprene oxidation
277 mechanisms for global atmospheric modelling, *J. Atmos. Chem.*, 37 (1), 29–52.

278 Rayner, N. A., et al., (2003), Global analyses of sea surface temperature, sea ice, and night marine
279 air temperature since the late nineteenth century, *J. Geophys. Res.*, 108, 4407,
280 doi:10.1029/2002JD002670.

281 Shindell, D.T., et al., (2006), Multimodel simulations of carbon monoxide: Comparison with
282 observations and projected near future changes, *J. Geophys. Res.*, 111, D19306,
283 doi:10.1029/2006JD007100.

284 Da Silva, G., et al., (2010), Unimolecular β hydroxyperoxy radical decomposition with OH recycling
285 in the photochemical oxidation of isoprene, *Environ. Sci. Technol.*, 44, 250–256.

286 Stavrou, T., J. Peeters, and J.-F. Müller, (2010), Improved global modelling of HO_x recycling in

287 isoprene oxidation: evaluation against the GABRIEL and INTEX-A aircraft campaign
288 measurements, *Atmos. Chem. Phys.*, 10, 9863-9878, doi:10.5194/acp-10-9863-2010.

289 Stevenson, D.S., et al., (2006), Multimodel ensemble simulations of present-day and near-future
290 tropospheric ozone, *J. Geophys. Res.*, 111, D08301, doi:10.1029/2005JD006338

291 Tan, D., et al., (2001), HOx budgets in a deciduous forest: Results from the PROPHET summer
292 1998 campaign, *J. Geophys. Res.*, 106, 24,407–24,427

293 Telford, P.J., et al., (2010), Effects of climate-induced changes in isoprene emissions after the
294 eruption of Mount Pinatubo, *Atmos. Chem. Phys.*, 10, 7117-7125, doi:10.5194/acp-10-7117-2010.

295 Thompson, A. M., et al., (2003a), Southern Hemisphere Additional Ozonesondes (SHADOZ) 1998–
296 2000 tropical ozone climatology: 1. Comparison with Total Ozone Mapping Spectrometer (TOMS)
297 and ground-based measurements, *J. Geophys. Res.*, 108(D2), 8238, doi:10.1029/2001JD000967.

298 Thompson, A. M., et al., (2003b), Southern Hemisphere Additional Ozonesondes (SHADOZ)
299 1998–2000 tropical ozone climatology: 2. Tropospheric variability and the zonal wave-one, *J.*
300 *Geophys. Res.*, 108(D2), 8241, doi:10.1029/2002JD002241.

301 Wang K.-Y and D.E. Shallcross (2000), Modelling terrestrial biogenic isoprene fluxes and their
302 potential impact on global chemical species using a coupled LSM–CTM model. *Atmos. Environ.*,
303 34, 2909–2925.

304 Whalley, L.K., et al. (2010), The chemistry of OH and HO₂ radicals in the boundary layer over the
305 tropical Atlantic Ocean. *Atmos. Chem. Phys.*, 10, 1555-1576, doi:10.5194/acp-10-1555-2010.

306 Whalley, L.K., et al., (2011), Quantifying the magnitude of a missing hydroxy radical source in a
307 tropical rainforest, *in prep.*

308 Young, P.J., et al. (2009) The CO₂ inhibition of terrestrial isoprene emission significantly affects
309 future ozone projections. *Atmos. Chem. Phys.*, 9, 2793-2803, doi:10.5194/acp-9-2793-2009.

310

311 **Captions:**

312 Table 1. Prescribed methane levels (mixing ratios in ppmv) and emissions for the three sets of
313 simulations. All emissions are given as global yearly averages in Tg of species emitted. See text for
314 sources of emissions.

315

316 Table 2. Tropospheric burdens of O₃, OH and CO for each model run. Troposphere defined using
317 lapse rate tropopause (see Figure 2).

318

319 Figure 1. Comparison of PD results with observations. Panel (a) comparison with ozone-sonde data
320 (data from Logan [1999] and Thompson et al. [2003a, 2003b]). Panel (b) comparison with surface
321 CO measurements (data from the NOAA GMD network [Novelli et al., 1998]). Panel (c)
322 comparison with surface observations made during the OP3 campaign in Borneo. OH data are
323 measured using Leeds FAGE instrument [Whalley et al., 2010], RO₂+HO₂ are measured using
324 Leicester PERCA instrument [Fleming et al., 2006]. In all cases observations are given by black
325 lines and symbols, with the PD-B data given by red lines and dots and the PD-M data by blue lines
326 and dots. Sensitivity simulations are shown in Panel (c) for reducing the rates of k_1+k_2 by half
327 (green lines).

328

329 Figure 2. Multiannual mean surface (less than 600m) and zonal changes in OH, CO and O₃ between
330 Modified run and Base run for three climate/emission scenarios. Changes in O₃ and CO are
331 expressed as absolute changes (Mod-Base), changes in OH presented as percentage changes ((Mod-
332 Base)/Base)×100. Surface changes shown for PD conditions only. Zonal plots have the respective
333 height of the tropopause superimposed (thick black dashed line) for each scenario (Note figures are
334 clipped in height to focus attention on the effects in the troposphere.).

335

336 **Tables and Figures:**

337 Table 1.

	NO ₂	CO	HCHO	C ₂ H ₆	C ₃ H ₈	Acetone	CH ₃ CHO	C ₅ H ₈	CH ₄
PI (1860)	34.3	434.7	4.1	10.2	3.7	43.8	6.7	573	0.790
PD (2000)	147	1078.1	6.3	51.1	48.5	65.3	24.2	467.1	1.655
FC (2100)	122.9	1039.5	5.7	45.8	42.3	63.1	22.4	545.3	2.973

338

339

340

341

342

343

344

345 Table 2.

Run	Ozone Burden (Tg)	OH Burden (Tg)	CO Burden (Tg)
PI-B	194	7.74×10^{-5}	347
PI-M	230	1.16×10^{-4}	280
PD-B	323	1.15×10^{-4}	432
PD-M	348	1.34×10^{-4}	404
FC-B	347	1.04×10^{-4}	567
FC-M	380	1.21×10^{-4}	543

346

347